Sensors and Actuators B 178 (2013) 113–118

Contents lists available at SciVerse ScienceDirect

Sensors and Actuators B: Chemical

journal homepage: www.elsevier.com/locate/snb

An amperometric biosensor based on human cytochrome P450 2C9 in polyacrylamide hydrogel films for bisphenol A determination

Pengyu Sun, Yunhua Wu*

Key Lab for Biotechnology of National Commission for Nationalities, College of Life Science, South Central University for Nationalities, Wuhan 430074, PR China

ARTICLE INFO

Article history:
Received 23 October 2012
Received in revised form
11 December 2012
Accepted 15 December 2012
Available online 22 December 2012

Keywords:
Cytochrome P450 2C9
Bisphenol A
Direct electron transfer
Biosensor

ABSTRACT

Electrochemical behavior of human cytochrome P450 2C9 (CYP2C9) incorporated in polyacrylamide (PAM) hydrogel films cast on glassy carbon electrodes (GCE) was investigated. CYP2C9–PAM film electrodes showed a pair of well-defined and nearly reversible cyclic voltammetric peaks. The electron-transfer rate constant was about 6.96 s^{-1} in pH 7.0 buffers, and the formal potential ($E^{0\prime}$) was −0.427 V (vs. SCE). The dependence of $E^{0\prime}$ on solution pH indicated that one-proton transfer was coupled to each electron transfer in the direct electron-transfer reaction. UV–vis absorption spectroscopy demonstrated that CYP2C9 retained a near native conformation in PAM films at medium pH. The CYP2C9 in the PAM film retained its bioactivity and could catalyze the reduction of dissolved oxygen. Upon the addition of its substrate bisphenol A (BPA) to the air-saturated solution, the reduction peak current of dissolved oxygen increased, which indicates the catalytic behavior of CYP2C9 to BPA. By amperometry a calibration linear range for BPA was obtained to be 1.25–10.0 μM with a sensitivity of 18.21 μA mM^{-1}. And the apparent Michaelis–Menten constant for the electrocatalytic activity of CYP2C9 was estimated to be 3.90 μM for BPA.

1. Introduction

Bisphenol A (4,4′-isopropylidenediphenol, BPA), as an industrial chemical, is used in the manufacture of polycarbonate, epoxy resin and numerous plastic articles [1]. These final products are widely utilized in food and drink storage containers, polycarbonate baby bottles, tableware, white dental fillings and sealants. BPA will inevitably migrate into food and beverage from packing of product, and then humans may routinely ingest trace amounts of BPA. Gaido et al. [2] had reported that BPA has estrogenic activity, and demonstrated developmental and reproductive toxicities in rats and mice fed at high-doses, with particularly strong effects in fetuses [3]. Sugita-Konishi et al. recently reported that BPA possesses immunotoxicity and reduces the non-specific host defense to a level that causes acute toxicity in mice [4].

Cytochrome P450 (CYP) comprises a superfamily of enzymes that catalyze the oxidation of a wide variety of xenobiotic chemicals including drugs, carcinogens, and steroids including sex hormones [5]. It was reported that CYPs are closely associated with the metabolism and toxicity of BPA in rats. BPA is metabolized to DNA-reactive bisphenol-*o*-quinone through 5-hydroxybisphenol and bisphenol semiquinone in rats [6]. Metabolism and interaction of bisphenol A in human hepatic cytochrome P450 have been studied. The results showed that BPA was predominantly metabolized by the CYP 2C subfamily (CYP2C9, CYP 2C18, and CYP 2C19) in human liver [7].

Since CYP 450 catalysis is an electron-transfer (ET)-chain, it might be suitable to substitute the biological electron delivery system completely by an electrode. In the previous years, the electrochemical properties of the various isoforms of CYP have been investigated. Direct electrochemistry and catalysis of P450BM3 [8], human 1A2 [9], human 2B6 [10], human 2E1[11], human 3A4 [12], house fly cytochrome P450 6A1 [13] and rat cytochrome P450 1A1[14] have been shown on modified electrodes. In addition, two reviews on P450 biosensors have also appeared [15,16]. These studies showed that P450 biosensors may be potential alternatives that would allow quick measurements for many compounds with comparative simple equipments.

In this work, human cytochrome P450 2C9 was incorporated into polyacrylamide (PAM) film to study its direct electrochemistry and electrocatalysis to bisphenol A. PAM hydrogels are obtained by free radical cross linking copolymerization of acrylamide and N,N-methylenebis(acrylamide) monomers with many hydrophilic amide groups. It was widely used in the field of life science. The hydrogel can form a stable film on electrode surface, which provide a microenvironment for CYP2C9. The direct electron transfer between the immobilized CYP2C9 and the electrode was achieved and an amperometric biosensor based on cytochrome p450 2C9 for bisphenol A sensing was developed.

* Corresponding author. Tel.: +86 27 8750 6365; fax: +86 27 6784 2689.
E-mail address: yunhuawu@yahoo.com.cn (Y. Wu).

0925-4005/$ – see front matter © 2013 Elsevier B.V. All rights reserved.
http://dx.doi.org/10.1016/j.snb.2012.12.055

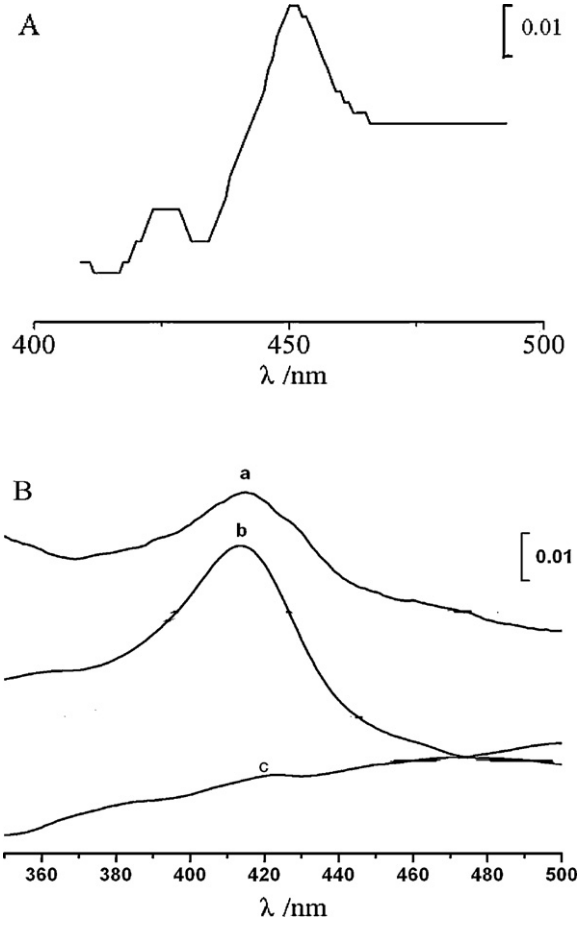

Fig. 1. (A) Fe^{2+}-CO vs. Fe^{2+} difference spectra of CYP2C9 expressed in *E. coli* cells after purification. For spectral analysis, samples were diluted in 100 mM Tris–HCL pH 7.4, containing 20% glycerol (v/v), and 1 mM EDTA. (B) UV–vis absorption spectra of (a) dry CYP2C9–PAM film, (b) dry CYP2C9 film and (c) dry PAM film on optical glass plates.

2. Experimental

2.1. Materials

Human cytochrome P450 2C9 was expressed in *Escherichia coli* and purified in our lab [13]. CYP2C9 concentration was determined by the general method of Omura and Sato using an extinction coefficient of 91 mM^{-1} cm^{-1} [17] based on the CO-difference spectrum (A in Fig. 1). Acrylamide, N,N′-methylenebisacrylamide and bisphenol A were obtained from Sigma. Buffers were 0.1 M Na_2HPO_4 and NaH_2PO_4 and its pH were adjusted with HCl or NaOH solutions. All other chemicals were of analytical grade and used as obtained. All solutions were prepared with twice-distilled water.

2.2. Preparation of the enzyme electrode

The glassy carbon electrode (GCE) with the diameter of 3 mm was used as the working electrode. The active area of a glassy carbon electrode with diameter 3 mm was determined by cyclic voltammmetry using the Randles–Sevcik equation for a reversible redox couple $[Fe(CN)_6]^{3-}/[Fe(CN)_6]^{2-}$ with a value about 4.78 mm^2. The electrode was first polished with 0.05 μm alumina slurry, then sonicated in nitric acid (1:1), ethanol and twice distilled water in turn. 30% polyacrylamide aqueous solution was obtained by dissolving 2.9 g acrylamide and 0.1 g N,N′-methylenebisacrylamide in 10 mL distilled water. It was stored at room temperature after filtration with 0.45 μm filtering membrane. To prepare the CYP2C9 incorporated PAM modified electrode (CYP2C9–PAM/GCE), 5 μL 30% polyacrylamide aqueous solution, 5 μL CYP2C9 solution (0.1 mM) and 0.3 μL 10% ammonium persulfate solution was mixed together, thus, the total amount of protein coated on the electrode surface is 5×10^{-10} M. Then all of this mixture was drop-coated on the surface of the pretreated GCE. For control experiments, only 5 μL of the CYP2C9 solution or the PAM solution without the enzyme was directly drop-coated onto the surface of the pretreated GCE to produce P450 modified electrode (CYP2C9/GCE) or PAM modified electrode (PAM/GCE). All three electrodes were dried at room temperature for overnight to allow the formation of uniform interfaces.

2.3. Apparatus

Cyclic voltammetry (CV) was performed with a CHI660C electrochemical workstation (CHI Instruments, Shanghai, China). A three-electrode system, including a working CYP2C9–PAM film electrode, a saturated calomel electrode (SCE) and a platinum wire counter electrode, was employed. Prior to each experiment, the buffer solutions were purged with high-purity nitrogen for at least 30 min and a nitrogen environment was then kept over the solution in the cell. All experiments were carried out at room temperature. A UV-757CRT visible ultraviolet spectrophotometer (Shanghai Precision & Scientific Instrument Co., Ltd., China) equipped with 1.0 cm quartz cells was used for scanning the UV spectrum. Sample films for spectroscopy were prepared by dropping 10 μL of CYP2C9–PAM or CYP2C9 solution onto an optical glass slide and air-dried at room temperature. The reference was an uncoated glass slide.

3. Results and discussion

3.1. Direct electrochemistry of CYP2C9 immobilized in PAM film on the glassy carbon electrode

The position of the Soret absorption band in UV–vis absorption spectra can provide information about possible denaturation of heme proteins, and is a useful conformational probe for the study of heme proteins, especially for the study of conformational change in the heme group region [18]. Fig. 1B exhibits the UV–vis spectra of dry CYP2C9 and CYP2C9–PAM films. The Soret band of CYP2C9 in the PAM film is located at 415 nm (curve a). While, for dry CYP2C9 (curve b), the Soret band is located at 414 nm, suggesting that CYP2C9 embedded in PAM films do not cause conformational change in the heme group region.

SEM was used here to investigate the morphology of PAM film and CYP2C9–PAM film. Top views of PAM film on glassy carbon disk revealed that it forms a compact layer on the electrodes (Fig. 2A). However, CYP2C9–PAM film showed a quite different morphology, exhibiting a three-dimensional network porous structure with small particles (Fig. 2B). All this suggests that interactions between CYP2C9 and PAM govern the morphology of the dry films.

Fig. 3 shows the cyclic voltammograms of the GCE coated with PAM, the GCE covered with CYP2C9–PAM in 0.1 M oxygen-free pH 7.0 phosphate buffers. A pair of well-defined and nearly symmetrical redox peaks is observed at the CYP2C9–PAM/GCE electrode (curve b), while there are no redox peaks appeared at the PAM/GCE (curve a). This indicates that the redox peaks in curve b attribute to the electrochemical reaction of the P-FeII/P-FeIII couple of CYP2C9. The anodic peak potential (E_{pa}) and the cathodic peak potential (E_{pc}) are located at about −0.372 and −0.482 V at scan rate of 1 V s^{-1}, respectively. The formal potential ($E^{0\prime}$), defined as the average of E_{pa} and E_{pc}, is about −0.427 V. The separation of the peak potential (ΔE_p) is 110 mV and the ratio of the cathodic current over the anodic current is close to one. In the experiment it was found that no

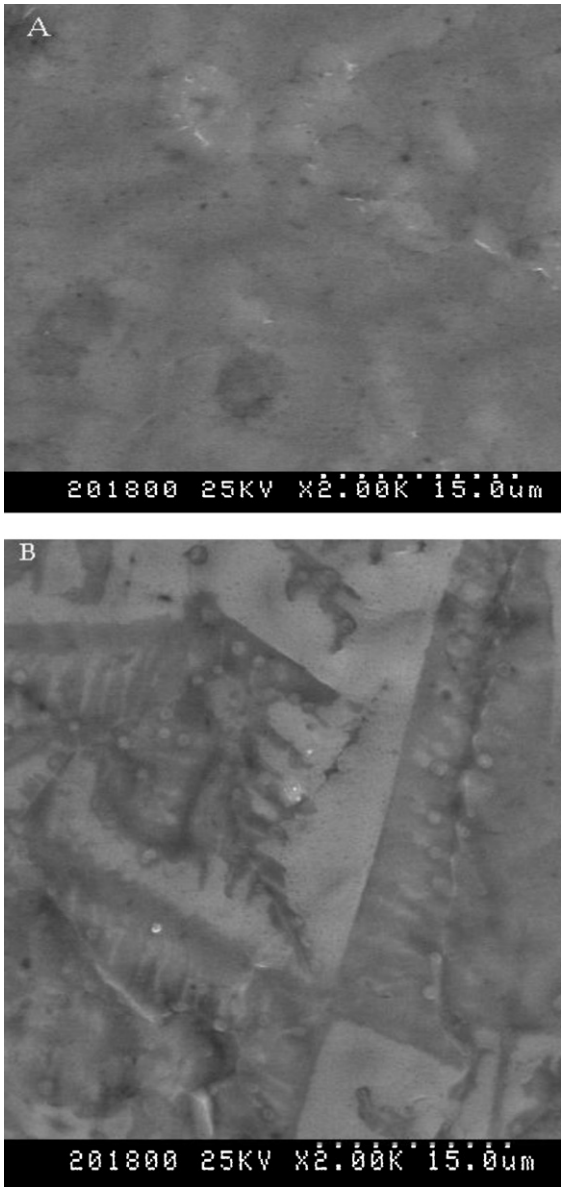

Fig. 2. SEM top views of (A) PAM film and (B) CYP2C9–PAM film on glassy carbon disks.

CV peaks were observed on CYP2C9/GCE, which demonstrates that PAM film facilitates the electrochemical communication between CYP2C9 and the electrode.

In the experiments it was found that there was no redox peaks when the bare GCE in CYP2C9 solution. Speculating upon the reason of the remarkably enhanced electron transfer rate of CYP2C9 in PAM, possible explanations include that CYP2C9 in PAM film keep its natural condition and maintain its activity. Adsorption of macromolecules can inhibit electron transfer between electrodes and proteins in solution [19]. So it contributes that PAM film adsorption can inhibit adsorption of CYP2C9 on the electrode and establish a viable pathway for electron transfer.

To obtain optimal cyclic voltammogram of CYP2C9 immobilized in PAM film, the effects of the concentration of PAM and the amount of the CYP2C9–PAM mixture applied to the GCE on the current responses were studied. When the concentration of PAM was 30%, maximal anodic current could be obtained. During the process of the modified electrode preparation, 10 μL of the CYP2C9–PAM mixture was cast onto the surface of the bare

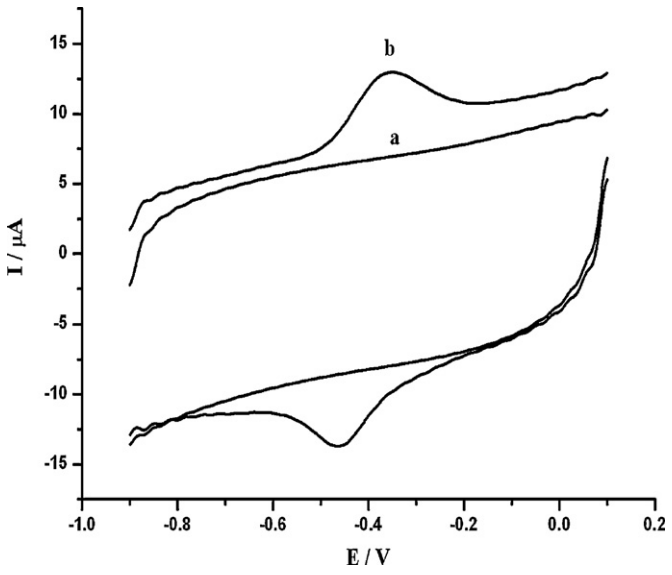

Fig. 3. Cyclic voltammograms of PAM/GCE (a); CYP2C9–PAM/GCE (b) in 0.1 M nitrogen-purged phosphate buffers (pH 7.0) at a scan rate of 1 V s^{-1}.

GCE to achieve maximal anodic current. Therefore, 30% PAM solution was mixed with CYP2C9 solution in 1:1 (v/v) ratio. And then 10 μL of the mixture was applied to the surface of the GCE to form the CYP2C9–PAM modified GCE in the following experiments. CVs of CYP2C9–PAM film had approximately symmetric peak shapes and nearly equal heights of reduction and oxidation peaks in the scan rates range from 1 V s^{-1} to 10 V s^{-1}. At scan rates lower than 1 V s^{-1}, reduction current is higher than oxidation current because of residue oxygen in CYP2C9–PAM film. Thus, 1 V s^{-1} was chosen in the following experiments. The cyclic voltammograms of CYP2C9/PAM/GCE at different scan rates are shown in Fig. 4A. Well-defined redox peaks could be obtained at scan rates ranging from 0.3 to 10 V s^{-1}. The reduction and oxidation peak currents exhibit good linear relationships with the scan rates (Fig. 4B). And the regression equations are $i_{pa}(\mu A) = 4.176 + 9.356\nu$ (V s^{-1}) ($r = 0.997$) and $i_{pc}(\mu A) = -6.042 + -7.396\nu$ (V s^{-1}) ($r = 0.995$). The integrations of cyclic voltammograms obtain a nearly constant charge Q at different scan rates. All these results suggest that the reaction was a surface-confined electrochemical behavior [20]. The surface coverage of the electroactive CYP2C9 (Γ) on CYP2C9–PAM/GCE was estimated from integration of the reduction peak in the CVs according to Laviron's equation [21]:

$$\Gamma = \frac{Q}{nFA} \quad (1)$$

where Q is the charge involved in the reaction, n the number of electron transferred, F Farady constant, and A the electrode area, with the result of 1.26×10^{-12} mol cm^{-2} for CYP2C9. These values are just about 2% of the total amount of protein coated on the electrode surface. This may suggest that only those enzymes in the inner layers of films closest to electrodes and with a suitable orientation can exchanges electrons with the electrodes and contribute to the observed redox reaction.

The kinetics of the heterogeneous electron transfer was analyzed using the model of Laviron [22]. For a peak separation <200 mV and the scan rate of 1 V s^{-1}, the electron transfer rate constant k_s can be estimated according to Laviron's equation:

$$k_s = \frac{mnF\nu}{RT} \quad (2)$$

where α is the transfer coefficient, k_s is the heterogeneous electron-transfer rate constant, m for CYP2C9 in this work is 0.18 according to ref. [22], n is the number of the number of electrons transferred in

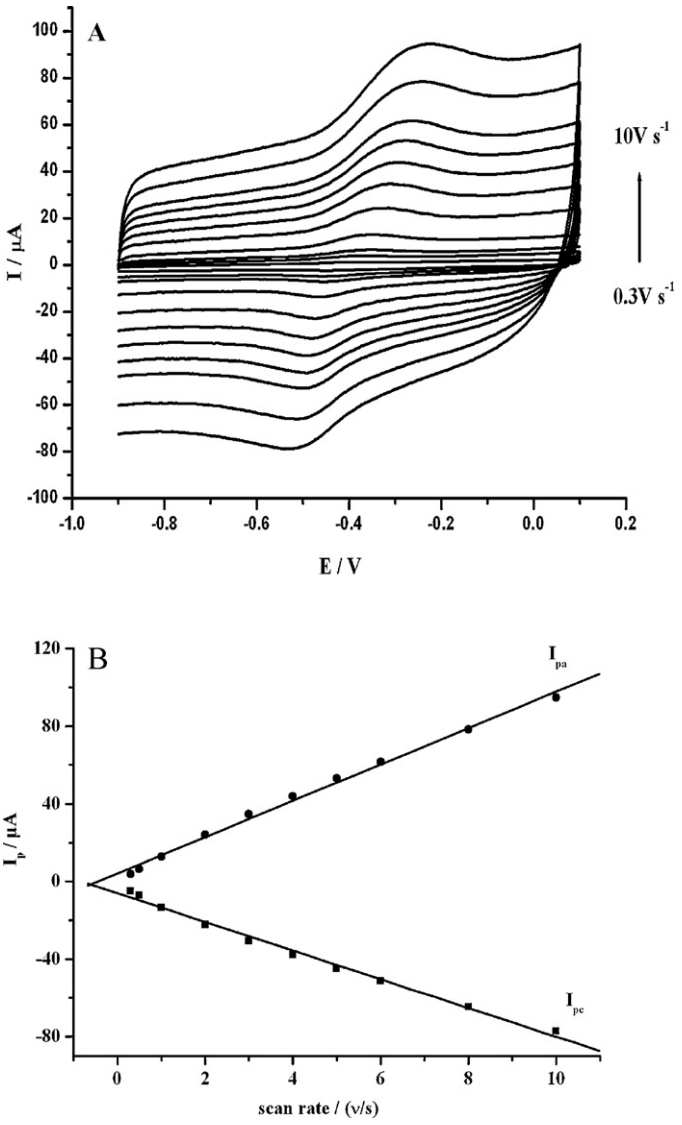

Fig. 4. (A) CYP2C9–PAM/GCE in 0.1 M nitrogen-purged phosphate buffers (pH 7.0) at various scan rates. (B) Plots of peak currents vs. scan rates.

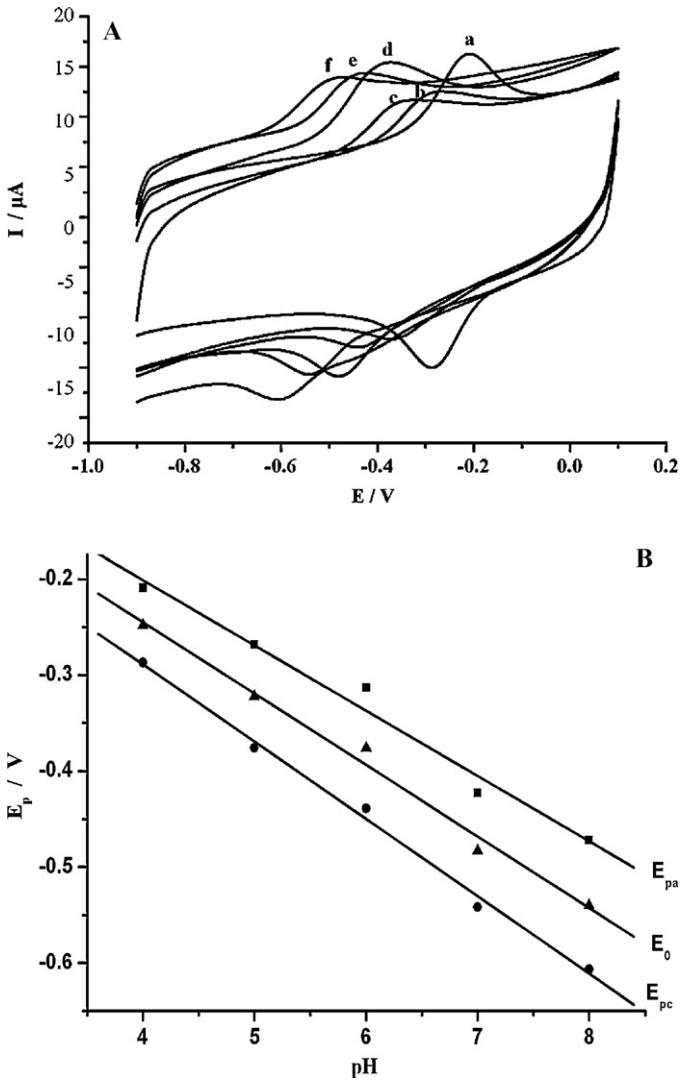

Fig. 5. (A) CYP2C9–PAM/GCE in 0.1 M nitrogen-purged phosphate buffers at various pH values: (a) 4.00; (b) 5.00; (c) 6.00; (d) 7.00; (e) 8.00; (f) 9.00. (B) Plots of oxidative peak potential E_{pa}, reductive peak potential E_{pc} and redox midpoint potential E_0' of CYP2C9–PAM/GCE vs. pH.

the rate-determining reaction, R is the gas constant, T is the absolute temperature, and ν is the scan rate. A graph of ΔE_p (the peak-to-peak separation) versus the logarithm of the scan rate yielded a straight line. Based on this, the values of $\alpha = 0.503$ and $k_s = 6.96\ s^{-1}$ were calculated. The value of k_s is greater than that identified as the lower limit for use as a bioelectrocatalyst [23], indicating good facilitation of the electron transfer between CYP2C9 and the electrode.

The pH of buffer solutions had significant influence on CV peak potentials of CYP2C9–PAM film (A in Fig. 5). Both reduction and oxidation peaks shifted negatively with increasing pH. In the pH range studied from 4 to 9, E_{pa}, E_{pc} and E_0' shifted to the negative direction with a slope of 52.4 mV pH^{-1}, 59.4 mV pH^{-1} and 56.7 mV pH^{-1}, respectively (B in Fig. 5). The E_0' values are smaller than the theoretically expected value of 59 mV pH^{-1} for the transfer of one proton and one electron per heme group during the electrode reaction [24], indicating that a single protonation accompanies the electron transfer of ferric ion in the active center of the protein (P-FeIII) to the electrodes. Thus, the simplified equation for the reduction of ferric ion of CYP2C9 in PAM film can be depicted as:

$$\text{P-FeIII} + H^+ + e^- \leftrightarrow \text{P-FeII} \quad (3)$$

The pH value also affects the redox peak current of CYP2C9 in PAM films (Fig. 5A). The peak currents at pH 5 and 6 are less than that at other pH values, indicating the amount of electroactive CYP2C9 molecule in PAM films decreases at pH 5 and 6. Maybe the conformation of CYP2C9 is influenced in such pH buffer. But it needs further investigation.

3.2. Catalytic activity of CYP2C9 in PAM film

Electrocatalytic reduction of oxygen by CYP2C9–PAM film was investigated by cyclic voltammetry (Fig. 6). When a certain amount of air was injected into pH 7.0 buffer solutions by a syringe, a marked increased in reduction peak at about −0.36 V was observed for CYP2C9–PAM film. However, direct reduction of O_2 was observed at PAM film at the potential −0.8 V. These results are characteristics of catalytic reduction O_2 by CYP2C9 confined in PAM film.

BPA is a potent endocrine disruptor, and widely spread in the environment. To develop a simple, general purpose BPA sensor that directly detects BPA is of significance. Here, the electrocatalytic oxidation of BPA was examined by cyclic voltammetry with CYP2C9–PAM film (Fig. 6). When BPA was added to 10 mL pH 7.0

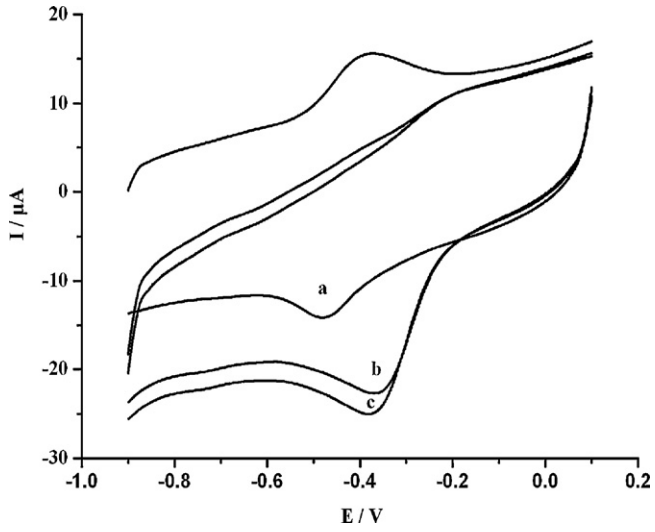

Fig. 6. Cyclic voltammograms of the CYP2C9–PAM/GCE in the nitrogen-purged pH 7.0 phosphate buffer (a), in the pH 7.0 phosphate air-saturated buffer (b), in the air-saturated pH 7.0 phosphate buffer after addition of 3.32 μM bisphenol A (c) at scan rate of 1 V s^{-1}, respectively.

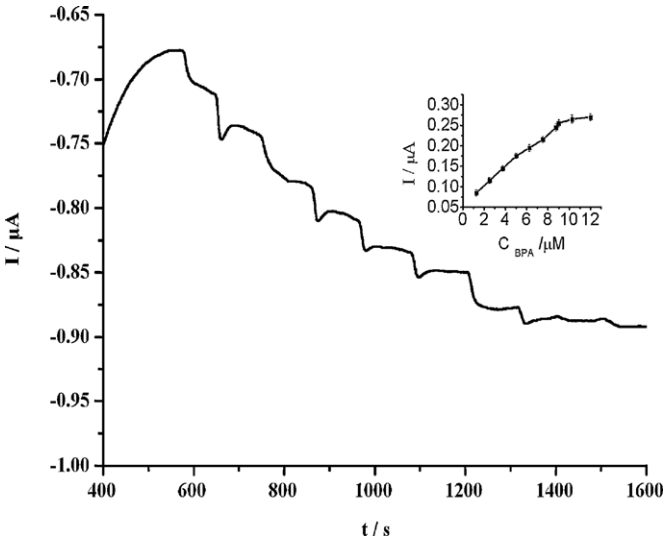

Fig. 7. Electrochemical responses at CYP2C9–PAM/GCE at −0.36 V in 8 mL of the pH 7.0 air-saturated phosphate buffer with injecting 10 μL of 1 mM BPA every 100 s. Inset: calibration curve of the reduction peak currents vs. the concentration of bisphenol A.

buffer, an increase of P-FeIII reduction peak at about −0.36 V was observed, accompanied by a decreased of P-FeII oxidation. The result indicated that a cycle catalytic reaction between P-FeII and BPA occurred and produced P-FeIII and hydroxylated BPA again [25]. To explain both the bioelectrocatalytic oxygen reduction current and the bioelectrocatalytic substrate conversion, a simplified reaction scheme was drawn that illustrates possible reaction ways (Scheme 1). Firstly, substrate ROH binds to ferric state of P450 (reaction (1)), the first electron is introduced (reaction (2)) followed by oxygen binding (reaction (3)). The ferrous dioxygen complex accepts a second electron (reaction (4)), and forms highly reactive peroxy intermediate. This intermediate accepts protons, producing a high-valence iron–oxygen complex, which is reactive enough to insert an oxygen atom into the substrate. Release of ROH (product) then restores the P450 to the starting ferric state (reaction (5)).

The current response of CYP2C9–PAM film to BPA was also studied by amperometric *i*–*t*. A current–time response of CYP2C9 on 8 successive step changes of BPA concentration is shown in Fig. 7. With the selected working potential −0.36 V, when an aliquot of BPA is added into the buffer solution, the reductive current increases and reaches the steady-state within 50 s, which indicates a fast diffusional process and a high activity of CYP2C9 in

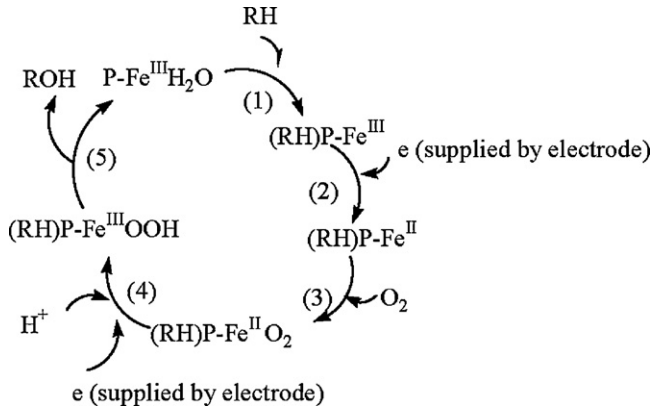

Scheme 1. General scheme of the electrocatalytic reaction of CYP2C9 in the presence of oxygen. The presence of bound substrate BPA is marked by (RH). P is for the protein.

PAM film. The calibration range of BPA is from 1.25 μM to 10.0 μM, with a regression equation of i_p(μA) = 0.075 + 0.018 C(μM) (r = 0.99, n = 14) (inset in Fig. 7). The detection limit was estimated to be 0.58 μM.

When the concentration of BPA in the electrochemical cell was higher than 10.0 μM, a plateau was observed, showing a characteristic of the Michaelis–Menten kinetic mechanism. The apparent Michaelis–Menten constant, K_m^{app}, which becomes a measure of the affinity of an enzyme for its substrate, can be obtained from the electrochemical version of the Lineweaver–Burk equation:

$$\frac{1}{I_{ss}} = \frac{1}{I_{max}} + \frac{K_m^{app}}{I_{max}C} \quad (4)$$

Here, I_{ss} is the steady-state current after the addition of substrate, C is the bulk concentration of the substrate, and I_{max} is the maximum current measured under saturated substrate conditions. The K_m^{app} value for the CYP2C9–PAM/GCE was found to be 3.90 μM [I^{-1}(μA) = 0.076 + 0.018 C^{-1}(μM), R = 0.997, n = 5], which is the same as that for the native NADPH-supported value 3.9 μM determined by HPLC method [7]. And it is indicated that the affinity of CYP2C9, which immobilized in PAM film, is not changed.

The BPA detection performances of the developed biosensor were compared with the other biosensors. The results were shown in Table 1. It can be seen that this is the first report that applied CYP2C9 to detect BPA and mostly other biosensors is based on tyrosinase. CYP2C9–PAM/GCE offered reasonable linear range for BPA detection and the detection limit was lower than some of previous reports.

CYP2C9 is recognized as one of the most important drug-metabolizing enzymes in humans [28] responsible for the hepatic clearance of S-warfarin, phenytoin, tolbutamide, torsemide and many non-steroidal anti-inflammatory agents [28]. Thus the selectivity of the proposed biosensor to BPA is not good, however, the proposed biosensor can be used as an amperometric detector coupled with HPLC to detect BPA. Furthermore, the proposed electrochemical biosensor can provide a platform to study the metabolism of CYP2C9 to BPA after electrolysis at −0.36 V with the aid of GC–MS.

The sensor showed good reproducibility for the determination of BPA concentration in the linear range. The variation coefficient was 2.3% for 7 successive assays of 2.5 μM BPA. The stability tests

Table 1
Performance comparison of the developed biosensor for BPA detection with other sensors.

Sensor	Linear range (μM)	Detection limit (μM)	References
Tyrosinase-MWCN paste electrode	1–16	1	[26]
Tyrosinase/CPE	1–20	0.15	[27]
Tyrosinase-SWCN paste electrode	0.1–12	0.02	[26]
Tyrosinase/CPE	0.1–15	0.1	[26]
CYP2C9–PAM/GCE	1.25–10	0.58	This work

were carried out at room temperature by measuring the response from day to day and the CYP2C9 biosensor was kept at room temperature. It was shown that the biosensor maintains its 92% initial activity after 10 days.

4. Conclusions

The direct electrochemistry and electrocatalysis to the bisphenol A of CYP2C9 were successfully realized by immobilizing CYP2C9 in polyacrylamide hydrogel film. In the presence of dissolved oxygen, the immobilized CYP2C9 displayed notably electrocatalytic responses to its substrate bisphenol A. The linear rang of the biosensor for bisphenol A was obtained by amperometry. Based on these results, an amperometric biosensor based on cytochrome p450 2C9 for bisphenol A determination was developed.

Acknowledgments

We gratefully acknowledge the financial support of the Hubei Provincial Natural Science Foundation (2011CDB423), the Special Fund for Basic Scientific Research of Central Colleges, South-Central University for Nationalities (CZZ11004).

References

[1] C.A. Staples, P.B. Dorn, G.M. Klecka, S.T.O. Block, L.R. Harris, A review of the environmental fate, effects and exposures of bisphenol A, Chemosphere 36 (2002) 2149–2173.
[2] K.W. Gaido, L.S. Leonard, S. Lovell, J.C. Gould, D. Babai, C.J. Portier, D.P. McDonnell, Evaluation of chemicals with endocrine modulating activity in a yeast-based steroid hormone receptor gene transcription assay, Toxicology and Applied Pharmacology 143 (1997) 205–212.
[3] J.C. Kim, H.C. Shin, S.W. Cha, W.S. Koh, M.K. Chung, S.S. Han, Evaluation of developmental toxicity in rats exposed to the environmental estrogen bisphenol A during pregnancy, Life Sciences 69 (2001) 2611–2625.
[4] Y. Sugita-Konishi, S. Shimura, T. Nishikawa, F. Sunaga, H. Naito, Y. Suzuki Y, Effect of bisphenol A on non-specific immunodefenses against non-pathogenic *Escherichia coli*, Toxicology Letters 136 (2003) 217–227.
[5] T. Niwa, Y. Yabusaki, K. Homma, N. Matsuo, K. Tatsuta, F. Ishibashi, M. Katagiri, Contribution of human hepatic cytochrome P450 isoforms to regioselective hydroxylation of steroid hormones, Xenobiotica 28 (1998) 539–547.
[6] A. Atkinson, D. Roy, In vivo DNA adduct formation by bisphenol A, Environmental and Molecular Mutagenesis 26 (1995) 60–66.
[7] N. Toshiro, F. Megumi, K. Kae, Y. Yoshiyasu, I. Fumihide, K. Masanao, Metabolism and interaction of bisphenol A in human hepatic cytochrome P450 and steroidogenic CYP17, Biological and Pharmaceutical Bulletin 24 (2001) 1064–1067.
[8] B.D. Fleming, Y.N. Tian, S.G. Bell, L.L. Wong, W. Urlacher, H.A.O. Hill, Redox properties of cytochrome P450 BM3 measured by direct methods, European Journal of Biochemistry 270 (2003) 4082–4088.
[9] S. Joseph, J.F. Rusling, Y.M. Lvov, T. Friedberg, U. Fuhr, human cytochrome P450 (CYP3A4) as a novel drug screening tool, Biochemical Pharmacology 65 (2003) 1817–1826.
[10] S.Q. Liu, L. Peng, X.D. Yang, Y.F. Wu, L. He, Electrochemistry of cytochrome P450 enzyme on nanoparticle-containing membrane-coated electrode and its applications for drug sensing, Analytical Biochemistry 375 (2008) 209–216.
[11] A. Fantuzzi, M. Fairhead, G. Gilardi, Direct electrochemistry of immobilized human cytochrome P450 2E1, Journal of the American Chemical Society 126 (2004) 5040–5041.
[12] C.Y. Dai, Y.L. Ding, M. Li, J.J. Fei, Direct electrochemistry of cytochrome P450 in a biocompatible film composed of an epoxy polymer and acetylene black, Microchimica Acta 176 (2012) 397–404.
[13] L. Zhang, X.Q. Liu, C.T. Wang, X.Q. Liu, G. Cheng, Y.H. Wu, Expression, purification and direct eletrochemistry of cytochrome P450 6A1 from the house fly, *Musca domestica*, Protein Expression and Purification 71 (2010) 74–78.
[14] Y.H. Wu, X.Q. Liu, L. Zhang, C.T. Wang, An amperometric biosensor based on rat cytochrome P450 1A1 for benzo[*a*]pyrene determination, Biosensors and Bioelectronics 26 (2011) 2177–2182.
[15] N. Bistolas, U. Wollenbergera, C. Jungb, F.W. Scheller, Cytochrome P450 biosensors—a review, Biosensors and Bioelectronics 20 (2005) 2408–2423.
[16] E. Schneider, D.S. Clark, Cytochrome P450 (CYP) enzymes and the development of CYP biosensors, Biosensors and Bioelectronics 39 (2013) 1–13.
[17] T. Omura, R. Sato, The carbon monoxide-binding pigment of liver microsomes, Journal of Biological Chemistry 239 (1964) 2370–2378.
[18] P. George, G.I.H. Hanania, Spectrophotometric study of ionizations in methemoglobin, Biochemical Journal 55 (1953) 236–243.
[19] Z. Zhang, J.F. Rusling, Electron transfer between myoglobin and electrodes in phosphatidyl choline and dihexadecyl phosphate films, Biophysical Chemistry 63 (1997) 133.
[20] R.W. Murray, in: A.J. Bard (Ed.), Electroanalytical Chemistry, vol. 13, Marcel Dekker, New York, 1984, pp. 191–368.
[21] A.E.F. Nassar, W.S. Willis, J.F. Rusling, Electron transfer from electrodes to myoglobin: facilitated in surfactant films and b locked by adsorbed biomacromolecules, Analytical Chemistry 67 (1995) 2386–2392.
[22] E. Laviron, General expression of the linear potential sweep voltammogram in the case of diffusionless electrochemical systems, Journal of Electroanalytical Chemistry 101 (1979) 19–28.
[23] B. Munge, C. Estavillo, J.B. Schenkman, J.F. Rusling, Optimization of electrochemical and peroxide-driven oxidation of styrene with ultrathin polyion films containing cytochrome P450cam and myoglobin, ChemBioChem 4 (2003) 82–89.
[24] A.M. Bond, Modern Polarographic Methods in Analytical Chemistry, Marcel Dekker, New York, 1980, pp. 27–45.
[25] I.G. Denisov, T.M. Makris, S.G. Sligar, I. Schlichting, Structure and chemistry of cytochrome P450, Chemical Reviews 105 (2005) 2253–2277.
[26] D. Mita, A. Attanasio, F. Arduini, N. Diano, V. Grano, U. Bencivenga, S. Rossi, A. Amine, D. Moscone, Enzymatic determination of BPA by means of tyrosinase immobilized on different carbon carriers, Biosensors and Bioelectronics 23 (2007) 60–65.
[27] S. Andreescu, O. Sadik, The correlation of analyte structures with biosensor responses using structure–activity relationship: detection of phenolic estrogens as model, Analytical Chemistry 76 (2004) 552–560.
[28] J.O. Miners, D.J. Birkett, Cytochrome P450 2C9: an enzyme of major importance in human drug metabolism, British Journal of Clinical Pharmacology 45 (1998) 525–538.

Biographies

Pengyu Sun studied in South-Central University for Nationalities from 2010 for bachelor degree, and majored in cytochrome P450s-based electrochemical biosensor.

Yunhua Wu graduated from South-Central University for Nationalities in 1992, and took PhD in chemistry from Wuhan University in 2006. At present, she is an associate professor at the College of Life-Science of South Central University for Nationalities, China. Research field of interest is in electrochemical biosensor.